Indian Journal of Geo Marine Sciences
Vol. 50 (11), November 2021, pp. 969-977

Single beacon underwater navigation method in the presence of unknown effective sound velocity, clock drift and inaccurate beacon position

X Yu, H-D Qin & Z-B Zhu*
Science and Technology on Underwater Vehicle Laboratory, Harbin Engineering University, Harbin – 150 001, China
*[E-mail: zhuzhongben@hrbeu.edu.cn]

Received 31 August 2021; revised 30 November 2021

Existing single beacon navigation systems commonly require precise known Effective Sound Velocity (ESV) and beacon position, as well as clock synchronization between the beacon and the hydrophone. However, these conditions are often difficult to guarantee in practical applications. Unknown clock drift, inaccurate ESV and beacon position will affect the range measurement precision, and consequently induce large localization errors. To eliminate the influence of above mentioned factors on the positioning accuracy, this paper proposes a new method of single beacon navigation. It treats clock drift, ESV and beacon position as unknown system parameters, and estimates them by the Expectation Maximization (EM) method. The advantages of new method are verified by field data. Numerical examples indicate that the method has better navigation performance than existing state-of-the-art methods in the presence of unknown clock-drift, ESV and beacon position setting error.

[**Keywords**: Clock drift, Effective sound velocity; Expectation-maximization; Single beacon navigation]

Introduction

In the past several decades, the Autonomous Underwater Vehicles (AUVs) have played a crucial role in civilian and military applications, such as the underwater operation, environmental inspection, maritime search and rescue[1-3]. Accurate position perception is an essential condition for AUVs to complete the predetermined underwater tasks. Because Global Navigation Satellite System (GNSS) signals are not available underwater, underwater navigation is extremely challenging. There are two main categories of commonly used underwater navigation methods: the dead reckoning using proprioceptive sensing and the acoustic navigation aided by acoustic signal. Dead reckoning predicts the new position relative to previous position fix by depending on the estimates of AUV velocity and travel time. Unbounded cumulative position error is common in dead reckoning method, which restricts its practical application in long-term underwater operation. The localization of acoustic navigation technology is achieved by the range/range differences measured by the Time of Arrival (TOA)/ Time Differences of Arrival (TDOA) of acoustic signals. The most common method is Long Baseline (LBL) localization system, which provides a position fix by the acoustics triangular measurement from widely spaced fixed beacons. Typically, the LBL system is used for relatively wide area coverage navigation, and the positioning error is in meters. However, the expense and time of establishing an acoustic network limit the utilization of LBL system[4-5]. In addition to LBL system, the single beacon navigation method, which fuses the dead reckoning data and slant-range information from a single beacon, also has attracted the attention of researchers. Comparing with dead reckoning and LBL system, single beacon navigation method has bounded positioning error and better flexibility, which improve its application potential in underwater navigation.

Considerable research efforts have been devoted to single beacon underwater navigation[6-15]. Larsen[6] proposed the concept of synthetic LBL system that incorporates dead reckoning data and range and/or range rate measurements of single acoustic beacon. Similarly, Lee *et al.*[7] proposed the single beacon navigation model based on the combination of Inertial Measurement Unit (IMU), Doppler Velocity Log (DVL), depth sensor and single range measurement. Jin *et al.*[8] combined the concept of synthetic LBL system with Ultra-Short Baseline (USBL) system, and proposed a novel single beacon navigation system. The vehicle is equipped with IMU and multiple hydrophones, and uses the range difference measurements to correct the dead reckoning data through Kalman filter. Rypkema *et al.*[9] proposed a similar navigation system, in which the vehicle-mounted hydrophone array is used to acquire the acoustic range and angle measurements from AUV to single acoustic beacon, so as to realize self-localization.

Positioning error of single beacon navigation system mainly comes from three sources: 1) The Effective Sound Velocity (ESV) setting error. Because of the multi-path propagation of acoustic signal and the variations in water temperature, pressure, and salinity, ESV is location-correlated and difficult to determine precisely. The ESV setting error will lead to large range measurement error, and accordingly cause large localization error. 2) The unknown clock-drift. Accurate acoustic transit time depends on accurate clock synchronization between the clock of beacon and the core clock of AUV. This is commonly realized by synchronizing the beacon and AUV to the GNSS time before each operation. However, for the AUVs need to stay in the underwater environment for a long time, the amount of clock-drift during that time scale is noteworthy[16]. For instance, the Woods Hole Oceanographic Institute (WHOI) micro-modem, which is widely used in the single beacon navigation system, has a average clock drift of 162 microseconds per hour[17]. This represents that if the task lasts more than an hour, the unknown clock drift can be a remarkable source of error[17]. 3) The beacon position setting error. The estimation of AUV position depends on accurate beacon position, which requires calibration before performing the task. Commonly, the beacon is deployed on the surface vehicle, and its position is estimated through the range measurements between the beacon and the vehicle at different locations[18]. Any error in the calibration will directly affect the AUV navigation performance. All the single beacon navigation systems proposed[6-9] assume that ESV and beacon position are precisely known, and are based on the precise clock synchronization. These unrealistic assumptions will affect the practical performance of the single beacon navigation system.

Zhu *et al.*[10-15] treated the ESV and acoustic transit time as the state variable and measurement variable, respectively, and proposed the single beacon navigation model to estimate unknown ESV. Literature[10-15] indicates that the model exhibits good navigation performance. However, unknown clock drift and inaccurate beacon position were not considered in Zhu & Hu[10], Zhu *et al.*[11,12], Qin *et al.*[13], Yu *et al.*[14] and Deng *et al.*[15]. In addition to the single beacon navigation, some existing researches about the LBL localization system also considered unknown clock drift, inaccurate ESV and beacon positions. Batista proposed the LBL localization model with clock drift and inaccurate ESV[19]. The additive and multiplicative factors were introduced to compensate the influence of clock drift and inaccurate ESV, respectively. Olson *et al.*[20] considered the unknown beacon positions in the LBL system. Beacon positions were augmented as state variables, and were determined in the navigation process by voting scheme[20]. Both of above systems need multi-beacon range measurement, and both do not consider unknown clock drift, inaccurate ESV and beacon positions simultaneously. In practical underwater tasks, the navigation system proposed in literature[10-15,19,20] may have large positioning error induced by one or two error sources. To the knowledge of the authors, the published literatures on designing the single beacon navigation method do not consider the effect of unknown clock drift, inaccurate ESV and beacon position simultaneously.

Based on the Expectation Maximization (EM) method[2,21-26], a single beacon navigation method was proposed in the case of unknown clock drift, inaccurate ESV and beacon position in this paper. The unknown clock drift, ESV and beacon position are treated as system parameters and iteratively estimated through EM method. Since both the clock drift and the ESV are dynamic in practice, the online version of the EM method[26] will be utilized to estimate time-varying system parameters. Navigation performance of the proposed single beacon navigation method will be demonstrated by filed data.

Materials and Methods

In this section, the EM method will be utilized to eliminate the influence of unknown clock drift, inaccurate ESV and beacon position.

Single beacon underwater navigation model

The kinematic and measurement models of the single beacon navigation system are reviewed in this part. The reader can refer to Zhu & Hu[10] and Gadre & Stilwell[27] for model details. Based on the assumption that the ocean current and the in-water velocity of the vehicle are constant within the discrete-time interval Δt, the discrete-time kinematic model of the single beacon navigation is as follows:

$$\underbrace{\begin{bmatrix} x_{k+1} \\ y_{k+1} \\ v_{cx,k+1} \\ v_{cy,k+1} \end{bmatrix}}_{\mathbf{x}_{k+1}} = \underbrace{\begin{bmatrix} 1 & 0 & \Delta t & 0 \\ 0 & 1 & 0 & \Delta t \\ 0 & 0 & 1 & 0 \\ 0 & 0 & 0 & 1 \end{bmatrix}}_{\mathbf{A}_k} \underbrace{\begin{bmatrix} x_k \\ y_k \\ v_{cx,k} \\ v_{cy,k} \end{bmatrix}}_{\mathbf{x}_k} + \underbrace{\begin{bmatrix} \Delta t & 0 \\ 0 & \Delta t \\ 0 & 0 \\ 0 & 0 \end{bmatrix}}_{\mathbf{B}_k} \underbrace{\begin{bmatrix} v_{wx,k} \\ v_{wy,k} \end{bmatrix}}_{\mathbf{u}_k} + \underbrace{\begin{bmatrix} w_{x,k} \\ w_{y,k} \\ w_{cx,k} \\ w_{cy,k} \end{bmatrix}}_{\mathbf{w}_k} \quad \ldots (1)$$

Where, x_k and y_k represent the horizontal coordinates of the hydrophone at epoch k; $v_{cx,k}$ and $v_{cy,k}$ represent the ocean current components in the x and y directions, respectively; $v_{wx,k}$ and $v_{wy,k}$ represent the in-water velocity components of the vehicle in the x and y directions, respectively; $\mathbf{x}_k, \mathbf{A}_k, \mathbf{B}_k$ and $\mathbf{u}_k$ represent the state vector, the system transition matrix, the control matrix and the input vector, respectively; $\mathbf{w}_k$ denotes the system uncertainty, which is modeled as a Gaussian white noise process. The vehicle speed $v_{w,k}$ can be estimated by the speed reading of the vehicle propeller. Combining $v_{w,k}$ with the vehicle heading φ_k measured by an electronic compass, $v_{wx,k}$ and $v_{wy,k}$ can be obtained through $v_{wx,k} = v_{w,k}\cos\varphi_k$ and $v_{wy,k} = v_{w,k}\sin\varphi_k$, respectively. Assuming that the two groups of uncertainty in $\mathbf{w}_k$ are mutually independent, the covariance matrix $\mathbf{Q}_k \in R^{4\times 4}$ for $\mathbf{w}_k$ can be characterized by two parameters: σ_c for the ocean current uncertainty, and σ_w for the vehicle in-water speed uncertainty. The specific expression of $\mathbf{Q}_k$ can be referred to sources Zhu & Hu[10] and Zhu *et al.*[11,12].

Most single beacon navigation systems treat the slant range as measurement variable[6-9], which is based on the assumption that the ESV and beacon position are precisely known, and the clock synchronization is accurate. To explicitly express the clock drift, ESV and beacon position in the measurement equation, we treat the acoustic transit time as measurement variable, and write the corresponding measurement equation as follows:

$$m_k = T_k^a - T_k^e = \frac{\sqrt{(x_k - x_b)^2 + (y_k - y_b)^2 + (z_k - z_b)^2}}{v_{e,k}} + \Delta T_k^t + v_{t,k} \quad \ldots (2)$$

Where, T_k^a and T_k^e denote the measured Time of Arrival (TOA) and the known Time of Emission (TOE), respectively; (x_k, y_k, z_k) and (x_b, y_b, z_b) are the coordinates of the vehicle and the beacon, respectively; $v_{e,k}$ denotes the ESV; ΔT_k^t denotes the clock drift; and $v_{t,k}$ denotes the measurement uncertainty associated with acoustic transit time. In this paper, both z_k and z_b are assumed as the known quantity obtained from depth sensors; $v_{t,k}$ is modeled as a zero-mean white Gaussian process with the variance $R_{t,k}$; x_b, y_b, $v_{e,k}$ and ΔT_k^t are all treated as unknown deterministic system parameters.

By denoting $\boldsymbol{\theta}_k = \left[x_b, y_b, v_{e,k}, \Delta T_k^t\right]^T$ as the unknown system parameter set, Eq. 2 can be written as follows:

$$m_k = h_k\left(\mathbf{x}_k, \boldsymbol{\theta}_k\right) + v_{t,k} \quad \ldots (3)$$

Where,

$$h_k(\mathbf{x}_k, \boldsymbol{\theta}_k) = \sqrt{(x_k - x_b)^2 + (y_k - y_b)^2 + (z_k - z_b)^2} \Big/ v_{e,k} + \Delta T_k^t$$

Online EM method

The online EM method stated in Huang[26] is used to estimate the $\boldsymbol{\theta}_k$ along with the state vector $\mathbf{x}_k$. The purpose of the EM method is to iteratively calculate $\boldsymbol{\theta}_k$ and $\mathbf{x}_k$, and get an increasingly good approximation of the Maximum Likelihood (ML) estimate. In the EM method, the cost function is defined as $Q\left(\boldsymbol{\theta}_k, \boldsymbol{\theta}_k^{(i)}\right)$, where $\boldsymbol{\theta}_k^{(i)}$ denotes an approximate value of estimated $\boldsymbol{\theta}_k$ at the ith step iteration. $Q\left(\boldsymbol{\theta}_k, \boldsymbol{\theta}_k^{(i)}\right)$ is defined as:

$$\begin{aligned} Q\left(\boldsymbol{\theta}_k, \boldsymbol{\theta}_k^{(i)}\right) &= \mathrm{E}_{\mathbf{x}_k}\left[\log p_{\boldsymbol{\theta}_k}\left(\mathbf{m}_{1:k}, \mathbf{x}_k\right) \middle| \boldsymbol{\theta}_k^{(i)}, \mathbf{m}_{1:k}\right] \\ &= \int \log p_{\boldsymbol{\theta}_k}\left(\mathbf{m}_{1:k}, \mathbf{x}_k\right) p_{\boldsymbol{\theta}_k^{(i)}}\left(\mathbf{x}_k \middle| \mathbf{m}_{1:k}\right) d\mathbf{x}_k \end{aligned} \quad \ldots (4)$$

Where, $\mathrm{E}_{\mathbf{x}}[\bullet]$ denotes an expectation with respect to $\mathbf{x}$; $\log(\bullet)$ represents the natural logarithmic function; $p_{\boldsymbol{\theta}}(\mathbf{a})$ represents the Probability

Distribution Function (PDF) of a random vector $\mathbf{a}$, which is dependent on the parameter $\boldsymbol{\theta}$; $\mathbf{m}_{1:k}$ represents the measurements from the first to the *k*th epoch; and $p(\mathbf{x} \mid \mathbf{y})$ is the condition probability of $\mathbf{x}$ given $\mathbf{y}$.

During each iteration, the approximation of estimated $\boldsymbol{\theta}_k$ can be written as the solution of following optimization problem[26]:

$$\boldsymbol{\theta}_k^{(i+1)} = \arg\max_{\boldsymbol{\theta}_k} Q\left(\boldsymbol{\theta}_k, \boldsymbol{\theta}_k^{(i)}\right) \quad \dots (5)$$

Denoting *N* as the total iteration times, the EM estimation of the unknown parameter $\boldsymbol{\theta}_k$ is

$$\hat{\boldsymbol{\theta}}_k = \boldsymbol{\theta}_k^{(N)} \quad \dots (6)$$

From Huang[26], the inequality

$$L_{\boldsymbol{\theta}_k}\left(\mathbf{m}_{1:k}\right) - L_{\boldsymbol{\theta}_k^{(i)}}\left(\mathbf{m}_{1:k}\right) \geq Q\left(\boldsymbol{\theta}_k, \boldsymbol{\theta}_k^{(i)}\right) - Q\left(\boldsymbol{\theta}_k^{(i)}, \boldsymbol{\theta}_k^{(i)}\right) \quad \dots (7);$$

always holds, in which $L_{\boldsymbol{\theta}_k}\left(\mathbf{m}_{1:k}\right) = \log p_{\boldsymbol{\theta}_k}\left(\mathbf{m}_{1:k}\right)$ is the cost function of ML method. Therefore, the $L_{\boldsymbol{\theta}_k}\left(\mathbf{m}_{1:k}\right)$ is non-decreasing as each iteration proceeds. Through calculating $Q\left(\boldsymbol{\theta}_k, \boldsymbol{\theta}_k^{(i)}\right)$ at E-step, and solving the optimization problem Eq. 5 at M-step iteratively, the EM method is formulated.

E-Step

$Q\left(\boldsymbol{\theta}_k, \boldsymbol{\theta}_k^{(i)}\right)$ is calculated in the E-step. Because process noise $\mathbf{w}_k$ and measurement noise $v_{t,k}$ are both assumed as white noise, the state is Markovian, and the measurement is conditional independent, $p_{\boldsymbol{\theta}_k}\left(\mathbf{m}_{1:k}, \mathbf{x}_k\right)$ can be decoupled[26] as:

$$p_{\boldsymbol{\theta}_k}\left(\mathbf{m}_{1:k}, \mathbf{x}_k\right) = p\left(\mathbf{x}_k \mid \mathbf{m}_{1:k-1}\right) p_{\boldsymbol{\theta}_k}\left(m_k \mid \mathbf{x}_k\right) p\left(\mathbf{m}_{1:k-1}\right) \quad \dots (8)$$

Due to the linearity of kinematic model, if the *a posterior* $p\left(\mathbf{x}_{k-1} \mid \mathbf{m}_{1:k-1}\right)$ is Gaussian, $p\left(\mathbf{x}_k \mid \mathbf{m}_{1:k-1}\right)$ will also be Gaussian[2]:

$$p\left(\mathbf{x}_k \mid \mathbf{m}_{1:k-1}\right) = N\left(\mathbf{x}_k; \hat{\mathbf{x}}_{k|k-1}, \mathbf{P}_{k|k-1}\right) \quad \dots (9)$$

Where, $N\left(\mathbf{x}; \boldsymbol{\mu}, \boldsymbol{\Sigma}\right)$ denotes the Gaussian PDF with mean vector $\boldsymbol{\mu}$ and covariance matrix $\boldsymbol{\Sigma}$. $\hat{\mathbf{x}}_{k|k-1}$ and $\mathbf{P}_{k|k-1}$ are the *a prior* state estimate and the *a prior* covariance matrix at the *k*th epoch, respectively, which can be directly obtained through the prediction procedure of the Kalman filter[10-12]:

$$\hat{\mathbf{x}}_{k|k-1} = \mathbf{A}_{k-1}\hat{\mathbf{x}}_{k-1|k-1} + \mathbf{B}_{k-1}\mathbf{u}_{k-1} \quad \dots (10)$$

$$\mathbf{P}_{k|k-1} = \mathbf{A}_{k-1}\mathbf{P}_{k-1|k-1}\mathbf{A}_{k-1}^T + \mathbf{Q}_{k-1} \quad \dots (11)$$

Where, $\hat{\mathbf{x}}_{k-1|k-1}$ and $\mathbf{P}_{k-1|k-1}$ are the *a posterior* state estimate and the *a posterior* covariance matrix at the *k-1*th epoch, respectively.

Since the measurement model $h_k\left(\mathbf{x}_k, \boldsymbol{\theta}_k\right)$ is nonlinear, conducting the linearization of $h_k\left(\mathbf{x}_k, \boldsymbol{\theta}_k\right)$ at the nominal point $\left(\overline{\mathbf{x}}_k, \overline{\boldsymbol{\theta}}_k\right)$, one gets

$$h_k\left(\mathbf{x}_k, \boldsymbol{\theta}_k\right) \approx h_k\left(\overline{\mathbf{x}}_k, \overline{\boldsymbol{\theta}}_k\right) + \mathbf{H}_{\mathbf{x}_k}\left(\mathbf{x}_k - \overline{\mathbf{x}}_k\right) + \mathbf{H}_{\boldsymbol{\theta}_k}\left(\boldsymbol{\theta}_k - \overline{\boldsymbol{\theta}}_k\right) \quad \dots (12)$$

Where,

$$\mathbf{H}_{\mathbf{x}_k} = \left.\frac{\partial h_k\left(\mathbf{x}_k, \boldsymbol{\theta}_k\right)}{\partial \mathbf{x}_k}\right|_{\mathbf{x}_k = \overline{\mathbf{x}}_k, \boldsymbol{\theta}_k = \overline{\boldsymbol{\theta}}_k}, \quad \mathbf{H}_{\boldsymbol{\theta}_k} = \left.\frac{\partial h_k\left(\mathbf{x}_k, \boldsymbol{\theta}_k\right)}{\partial \boldsymbol{\theta}_k}\right|_{\mathbf{x}_k = \overline{\mathbf{x}}_k, \boldsymbol{\theta}_k = \overline{\boldsymbol{\theta}}_k} \quad \dots (13)$$

are the Jacobians of the measurement model at the nominal point $\left(\overline{\mathbf{x}}_k, \overline{\boldsymbol{\theta}}_k\right)$. Using the linearized model Eq. 12, the likelihood PDF can be approximated by a Gaussian distribution:

$$p_{\boldsymbol{\theta}_k}\left(m_k \mid \mathbf{x}_k\right) = N\left(m_k; h_k\left(\overline{\mathbf{x}}_k, \overline{\boldsymbol{\theta}}_k\right) + \mathbf{H}_{\mathbf{x}_k}\left(\mathbf{x}_k - \overline{\mathbf{x}}_k\right) + \mathbf{H}_{\boldsymbol{\theta}_k}\left(\boldsymbol{\theta}_k - \overline{\boldsymbol{\theta}}_k\right), R_{t,k}\right) \quad \dots (14)$$

Substitute Eqs. 9 and 14 into Eq. 8, and conduct the logarithm operation. By neglecting the terms independent of $\boldsymbol{\theta}_k$, one gets

$$L_{\boldsymbol{\theta}_k}\left(\mathbf{m}_{1:k}, \mathbf{x}_k\right) = -0.5\left[m_k - h_k\left(\overline{\mathbf{x}}_k, \overline{\boldsymbol{\theta}}_k\right) - \mathbf{H}_{\mathbf{x}_k}\left(\mathbf{x}_k - \overline{\mathbf{x}}_k\right) - \mathbf{H}_{\boldsymbol{\theta}_k}\left(\boldsymbol{\theta}_k - \overline{\boldsymbol{\theta}}_k\right)\right]^2 R_{t,k}^{-1} + c_{\boldsymbol{\theta}_k} \quad \dots (15)$$

Where, $c_{\boldsymbol{\theta}_k}$ represents the constant value relative to variable $\boldsymbol{\theta}_k$.

Fix $\boldsymbol{\theta}_k^{(i)}$ and calculate the estimation of $\mathbf{x}_k$. Denote the *a posterior* PDF with parameter $\boldsymbol{\theta}_k^{(i)}$ as

$$p_{\boldsymbol{\theta}_k^{(i)}}\left(\mathbf{x}_k \mid \mathbf{m}_{1:k}\right) = N\left(\mathbf{x}_k ; \hat{\mathbf{x}}_{k|k}^{(i)}, \mathbf{P}_{k|k}^{(i)}\right) \quad \ldots (16)$$

Based on known $\boldsymbol{\theta}_k^{(i)}$, select $\hat{\mathbf{x}}_{k|k}^{(i-1)}$ as the nominal state and conduct the linearization of Eq. 3. The corresponding Jacobian is

$$\mathbf{H}_{\mathbf{x}_k}^{(i)} = \begin{bmatrix} \left(\hat{x}_{k|k}^{(i-1)} - x_b^{(i)}\right) \Big/ \left(v_{e,k}^{(i)} \sqrt{\left(\hat{x}_{k|k}^{(i-1)} - x_b^{(i)}\right)^2 + \left(\hat{y}_{k|k}^{(i-1)} - y_b^{(i)}\right)^2 + \left(z_k - z_b\right)^2}\right), \\ \left(\hat{y}_{k|k}^{(i-1)} - y_b^{(i)}\right) \Big/ \left(v_{e,k}^{(i)} \sqrt{\left(\hat{x}_{k|k}^{(i-1)} - x_b^{(i)}\right)^2 + \left(\hat{y}_{k|k}^{(i-1)} - y_b^{(i)}\right)^2 + \left(z_k - z_b\right)^2}\right), 0, 0 \end{bmatrix} \quad \ldots (17)$$

In the case that $\boldsymbol{\theta}_k^{(i)}$ is given, Eq. 3 is independent of $\boldsymbol{\theta}_k$. Therefore, $\mathbf{H}_{\boldsymbol{\theta}_k}\left(\boldsymbol{\theta}_k - \overline{\boldsymbol{\theta}}_k\right)$ on the right hand of Eq. 15 does not exist. Based on the Jacobian, the correction procedure of extended Kalman filter is utilized for calculating $p_{\boldsymbol{\theta}_k^{(i)}}\left(\mathbf{x}_k \mid \mathbf{m}_{1:k}\right)$ (refs. 10-12) as:

$$\mathbf{K}_k^{(i)} = \mathbf{P}_{k|k-1} \mathbf{H}_{\mathbf{x}_k}^{(i)T} \left(\mathbf{H}_{\mathbf{x}_k}^{(i)} \mathbf{P}_{k|k-1} \mathbf{H}_{\mathbf{x}_k}^{(i)T} + R_{t,k}\right)^{-1} \quad \ldots (18)$$

$$\hat{\mathbf{x}}_{k|k}^{(i)} = \hat{\mathbf{x}}_{k|k-1} + \mathbf{K}_k^{(i)} \left(m_k - h_k\left(\hat{\mathbf{x}}_{k|k}^{(i-1)}, \boldsymbol{\theta}_k^{(i)}\right) - \mathbf{H}_{\mathbf{x}_k}^{(i)}\left(\hat{\mathbf{x}}_{k|k-1} - \hat{\mathbf{x}}_{k|k}^{(i-1)}\right)\right) \quad \ldots (19)$$

$$\mathbf{P}_{k|k}^{(i)} = \mathbf{P}_{k|k-1} - \mathbf{K}_k^{(i)} \mathbf{H}_{\mathbf{x}_k}^{(i)} \mathbf{P}_{k|k-1} \quad \ldots (20)$$

Where, $\mathbf{K}_k^{(i)}$ is the Kalman gain.

Choosing $\left(\hat{\mathbf{x}}_{k|k}^{(i)}, \boldsymbol{\theta}_k^{(i)}\right)$ as the nominal point, $Q\left(\boldsymbol{\theta}_k, \boldsymbol{\theta}_k^{(i)}\right)$ can be calculated as:

$$Q\left(\boldsymbol{\theta}_k, \boldsymbol{\theta}_k^{(i)}\right) = -0.5 R_{t,k}^{-1} \int \left[m_k - h_k\left(\hat{\mathbf{x}}_{k|k}^{(i)}, \boldsymbol{\theta}_k^{(i)}\right) + \overline{\mathbf{H}}_{\mathbf{x}_k}^{(i)}\left(\mathbf{x}_k - \hat{\mathbf{x}}_{k|k}^{(i)}\right) + \overline{\mathbf{H}}_{\boldsymbol{\theta}_k}^{(i)}\left(\boldsymbol{\theta}_k - \boldsymbol{\theta}_k^{(i)}\right)\right]^2 \times N\left(\mathbf{x}_k ; \hat{\mathbf{x}}_{k|k}^{(i)}, \mathbf{P}_{k|k}^{(i)}\right) d\mathbf{x}_k + c_{\boldsymbol{\theta}_k} \quad \ldots (21)$$

Where, $\overline{\mathbf{H}}_{\mathbf{x}_k}^{(i)}$ and $\overline{\mathbf{H}}_{\boldsymbol{\theta}_k}^{(i)}$ are the Jacobian of $\hat{\mathbf{x}}_{k|k}^{(i)}$, and $\boldsymbol{\theta}_k^{(i)}$, respectively. By denoting

$$\hat{r}^{(i)} = \sqrt{\left(\hat{x}_{k|k}^{(i)} - x_b^{(i)}\right)^2 + \left(\hat{y}_{k|k}^{(i)} - y_b^{(i)}\right)^2 + \left(z_k - z_b\right)^2} \quad \ldots (22)$$

$\overline{\mathbf{H}}_{\mathbf{x}_k}^{(i)}$ and $\overline{\mathbf{H}}_{\boldsymbol{\theta}_k}^{(i)}$ can be written as

$$\overline{\mathbf{H}}_{\mathbf{x}_k}^{(i)} = \left[\left(\hat{x}_{k|k}^{(i)} - x_b^{(i)}\right) \Big/ \left(v_{e,k}^{(i)} \hat{r}^{(i)}\right) \quad \left(\hat{y}_{k|k}^{(i)} - y_b^{(i)}\right) \Big/ \left(v_{e,k}^{(i)} \hat{r}^{(i)}\right) \quad 0 \quad 0\right] \quad \ldots (23)$$

$$\overline{\mathbf{H}}_{\boldsymbol{\theta}_k}^{(i)} = \left[-\left(\hat{x}_{k|k}^{(i)} - x_b^{(i)}\right) \Big/ \left(v_{e,k}^{(i)} \hat{r}^{(i)}\right) \quad -\left(\hat{y}_{k|k}^{(i)} - y_b^{(i)}\right) \Big/ \left(v_{e,k}^{(i)} \hat{r}^{(i)}\right) \quad -\hat{r}^{(i)} \Big/ \left(v_{e,k}^{(i)}\right)^2 \quad 1\right] \quad \ldots (24),$$

respectively.

Simplify Eq. 21 as

$$Q\left(\boldsymbol{\theta}_k, \boldsymbol{\theta}_k^{(i)}\right) = -0.5 R_{t,k}^{-1} \left[\psi\left(\boldsymbol{\theta}_k, \boldsymbol{\theta}_k^{(i)}\right)^2 + \overline{\mathbf{H}}_{\mathbf{x}_k}^{(i)} \mathbf{P}_{k|k}^{(i)} \left(\overline{\mathbf{H}}_{\mathbf{x}_k}^{(i)}\right)^T\right] + c_{\boldsymbol{\theta}_k} \quad \ldots (25)$$

Where,

$$\psi\left(\boldsymbol{\theta}_k, \boldsymbol{\theta}_k^{(i)}\right) = m_k - \frac{\left(x_b^{(i)} - \hat{x}_{k|k}^{(i)}\right)\left(x_b - x_b^{(i)}\right) + \left(y_b^{(i)} - \hat{y}_{k|k}^{(i)}\right)\left(y_b - y_b^{(i)}\right)}{v_{e,k}^{(i)} \hat{r}^{(i)}} + \frac{\hat{r}^{(i)}\left(v_{e,k} - 2 v_{e,k}^{(i)}\right)}{\left(v_{e,k}^{(i)}\right)^2} - \Delta T_k^{t(i)} \quad \ldots (26)$$

M-Step

The maximum point of $Q\left(\boldsymbol{\theta}_k, \boldsymbol{\theta}_k^{(i)}\right)$ with respect to $\boldsymbol{\theta}_k$ will be found in the M-step. In this study, we will adopt the analytic method based on the calculation of stationary point. By maximum point definition, $\boldsymbol{\theta}_k^{(i+1)}$ should satisfy Frandsen *et al.*[28]:

$$\mathbf{J} = \left.\frac{\partial Q\left(\boldsymbol{\theta}_k, \boldsymbol{\theta}_k^{(i)}\right)}{\partial \boldsymbol{\theta}_k}\right|_{\boldsymbol{\theta}_k = \boldsymbol{\theta}_k^{(i+1)}} = \mathbf{0}_{1\times 4} \quad \ldots (27)$$

$$\mathbf{H} = \left.\frac{\partial^2 Q\left(\boldsymbol{\theta}_k, \boldsymbol{\theta}_k^{(i)}\right)}{\partial \boldsymbol{\theta}_k^2}\right|_{\boldsymbol{\theta}_k = \boldsymbol{\theta}_k^{(i+1)}} < 0 \quad \ldots (28)$$

Where, $\mathbf{0}_{1\times 4} \in =^{1\times 4}$ denotes zero vector, and $\mathbf{H} < 0$ denotes $\mathbf{H}$ is a negative definite matrix.

The first and second order derivatives of $Q\left(\boldsymbol{\theta}_k, \boldsymbol{\theta}_k^{(i)}\right)$ with respect to $\boldsymbol{\theta}_k$ are shown in Eqs. 29 and 30, respectively.

$$\mathbf{J} = -\frac{1}{R_{t,k}} \psi\left(\boldsymbol{\theta}_k, \boldsymbol{\theta}_k^{(i)}\right) \left[-\frac{x_b^{(i)} - \hat{x}_{k|k}^{(i)}}{v_{e,k}^{(i)} \hat{r}^{(i)}} \quad -\frac{y_b^{(i)} - \hat{y}_{k|k}^{(i)}}{v_{e,k}^{(i)} \hat{r}^{(i)}} \quad \frac{\hat{r}^{(i)}}{\left(v_{e,k}^{(i)}\right)^2} \quad -1\right] \quad \ldots (29)$$

$$\mathbf{H}=-\frac{1}{R_{t,k}}\begin{bmatrix} \frac{\left(x_b^{(i)}-\hat{x}_{k|k}^{(i)}\right)}{v_{e,k}^{(i)}\hat{r}^{(i)}}\frac{\left(x_b^{(i)}-\hat{x}_{k|k}^{(i)}\right)}{v_{e,k}^{(i)}\hat{r}^{(i)}} & \frac{\left(x_b^{(i)}-\hat{x}_{k|k}^{(i)}\right)}{v_{e,k}^{(i)}\hat{r}^{(i)}}\frac{\left(y_b^{(i)}-\hat{y}_{k|k}^{(i)}\right)}{v_{e,k}^{(i)}\hat{r}^{(i)}} & -\frac{\hat{r}^{(i)}}{\left(v_{e,k}^{(i)}\right)^2}\frac{\left(x_b^{(i)}-\hat{x}_{k|k}^{(i)}\right)}{v_{e,k}^{(i)}\hat{r}^{(i)}} & \frac{\left(x_b^{(i)}-\hat{x}_{k|k}^{(i)}\right)}{v_{e,k}^{(i)}\hat{r}^{(i)}} \\ \frac{\left(x_b^{(i)}-\hat{x}_{k|k}^{(i)}\right)}{v_{e,k}^{(i)}\hat{r}^{(i)}}\frac{\left(y_b^{(i)}-\hat{y}_{k|k}^{(i)}\right)}{v_{e,k}^{(i)}\hat{r}^{(i)}} & \frac{\left(y_b^{(i)}-\hat{y}_{k|k}^{(i)}\right)}{v_{e,k}^{(i)}\hat{r}^{(i)}}\frac{\left(y_b^{(i)}-\hat{y}_{k|k}^{(i)}\right)}{v_{e,k}^{(i)}\hat{r}^{(i)}} & -\frac{\hat{r}^{(i)}}{\left(v_{e,k}^{(i)}\right)^2}\frac{\left(y_b^{(i)}-\hat{y}_{k|k}^{(i)}\right)}{v_{e,k}^{(i)}\hat{r}^{(i)}} & \frac{\left(y_b^{(i)}-\hat{y}_{k|k}^{(i)}\right)}{v_{e,k}^{(i)}\hat{r}^{(i)}} \\ -\frac{\hat{r}^{(i)}}{\left(v_{e,k}^{(i)}\right)^2}\frac{\left(x_b^{(i)}-\hat{x}_{k|k}^{(i)}\right)}{v_{e,k}^{(i)}\hat{r}^{(i)}} & -\frac{\hat{r}^{(i)}}{\left(v_{e,k}^{(i)}\right)^2}\frac{\left(y_b^{(i)}-\hat{y}_{k|k}^{(i)}\right)}{v_{e,k}^{(i)}\hat{r}^{(i)}} & \frac{\hat{r}^{(i)}}{\left(v_{e,k}^{(i)}\right)^2}\frac{\hat{r}^{(i)}}{\left(v_{e,k}^{(i)}\right)^2} & \frac{\hat{r}^{(i)}}{\left(v_{e,k}^{(i)}\right)^2} \\ \frac{\left(x_b^{(i)}-\hat{x}_{k|k}^{(i)}\right)}{v_{e,k}^{(i)}\hat{r}^{(i)}} & \frac{\left(y_b^{(i)}-\hat{y}_{k|k}^{(i)}\right)}{v_{e,k}^{(i)}\hat{r}^{(i)}} & \frac{\hat{r}^{(i)}}{\left(v_{e,k}^{(i)}\right)^2} & 1 \end{bmatrix} \quad \ldots (30)$$

From Eq. 29, Eq. 27 is satisfied if and only if $\psi\left(\boldsymbol{\theta}_k,\boldsymbol{\theta}_k^{(i)}\right)=0$. Because there are four unknown parameters and one equality constraint, $\boldsymbol{\theta}_k$ has infinite solutions. Selecting ΔT_k^t as the variable, and choosing x_b, y_b and $v_{e,k}$ as their nominal values $\overline{x}_b$, $\overline{y}_b$ and $\overline{v}_{e,k}$ during the iteration process, one gets

$$\begin{aligned}\Delta T_k^{t(i+1)} &= m_k-\frac{\left(\overline{x}_b-\hat{x}_{k|k}^{(i)}\right)\left(\overline{x}_b-\overline{x}_b\right)+\left(\overline{y}_b-\hat{y}_{k|k}^{(i)}\right)\left(\overline{y}_b-\overline{y}_b\right)}{v_{e,k}^{(i)}\hat{r}^{(i)}}+\frac{\hat{r}^{(i)}\left(\overline{v}_{e,k}-2\overline{v}_{e,k}\right)}{\left(\overline{v}_{e,k}\right)^2} \\ &= m_k-\frac{\hat{r}^{(i)}}{\overline{v}_{e,k}}\end{aligned} \quad \ldots (31)$$

Combining Eqs. 27 and 31:

$$\begin{cases} x_b^{(i+1)}=\overline{x}_b, \\ y_b^{(i+1)}=\overline{y}_b, \\ v_{e,k}^{(i+1)}=\overline{v}_{e,k} \\ \Delta T_k^{t(i+1)}=m_k-\dfrac{\hat{r}^{(i)}}{\overline{v}_{e,k}} \end{cases} \quad \ldots (32)$$

Denote the leading principal minors of matrix $\mathbf{C}$ as $\mathbf{C}\left(1,2,\ldots p\right)$, $p=1,2,\ldots n$, which are the determinants of the upper left $p\times p$ submatrices of $\mathbf{C}$ (ref. 29). From Eq. 30, one gets

$$\begin{cases} -\mathbf{H}(1,1)=\dfrac{1}{R_{t,k}}\dfrac{\left(x_b^{(i)}-\hat{x}_{k|k}^{(i)}\right)^2}{\left(v_{e,k}^{(i)}\hat{r}^{(i)}\right)^2} \\ \mathbf{H}(1,2)=0, \\ -\mathbf{H}(1,2,3)=0, \\ \mathbf{H}(1,2,3,4)=0 \end{cases} \quad \ldots (33)$$

From Eq. 33 and Theorem 1.4 in Wilson[29], if $R_{t,k}$ is positive, then matrix $\mathbf{H}$ is negative semi-definite. Therefore, Eq. 28 is not satisfied, which means that Eq. 32 is not the maximum point of $Q\left(\boldsymbol{\theta}_k,\boldsymbol{\theta}_k^{(i)}\right)$. However, negative semi-definite matrix $\mathbf{H}$ ensures $Q\left(\boldsymbol{\theta}_k^{(i+1)},\boldsymbol{\theta}_k^{(i)}\right)\geq Q\left(\boldsymbol{\theta}_k^{(i)},\boldsymbol{\theta}_k^{(i)}\right)$ always holds. From Eq. 7, the measurement likelihood is still non-decreasing as each iteration proceeds, which indicates that it is reasonable to update the unknown parameters using Eq. 32.

Algorithm

Combing E-Step with M-Step, EM-based single beacon underwater navigation method at *k*th epoch is listed in Algorithm 1. In addition, we use indirect ocean current measurement to correct the ocean current[10-15] (the corresponding standard deviation of measurement noise is denoted as σ_{cm}). Specific correction steps can refer to literature[10-15], and are omitted for simplicity.

Results

The navigation performance of the proposed EM-based method (to be referred to as "PM") will be investigated by field data with unknown clock drift,

Algorithm 1 — EM-based single beacon navigation method with inaccurate ESV, beacon position and clock drift

Input: $\hat{\mathbf{x}}_{k-1|k-1},\mathbf{P}_{k-1|k-1},m_k,\overline{v}_{e,k},\overline{x}_b,\overline{y}_b,\Delta T_k^{t(0)}$.

1: Calculate $\hat{\mathbf{x}}_{k|k-1}$ and $\mathbf{P}_{k|k-1}$ through Eqs. 10 and 11, respectively.

2: Initialization: $\hat{\mathbf{x}}_{k|k}^{(0)}=\hat{\mathbf{x}}_{k|k-1}$, $\mathbf{P}_{k|k}^{(0)}=\mathbf{P}_{k|k-1}$.

3: Calculate $\hat{r}^{(0)}$ and $\Delta T_k^{t(1)}$ through Eqs. 22 and 31, respectively.

4: **for** $i=1$ to N **do**

5: Calculate $\mathbf{H}_{\mathbf{x}_k}^{(i)}$ through Eq. 17.

6: Calculate $\mathbf{K}_k^{(i)}$ and $\hat{\mathbf{x}}_{k|k}^{(i)}$ through Eqs. 18 and 19, respectively.

7: Calculate $\hat{r}^{(i)}$ and $\boldsymbol{\theta}_k^{(i+1)}$ through Eqs. 22 and 32, respectively.

8: **end for**

9: $\mathbf{P}_{k|k}^{(N)}=\mathbf{P}_{k|k-1}-\mathbf{K}_k^{(N)}\mathbf{H}_{\mathbf{x}_k}^{(N)}\mathbf{P}_{k|k-1}$.

10: $\hat{\mathbf{x}}_{k|k}=\hat{\mathbf{x}}_{k|k}^{(N)}$, $\mathbf{P}_{k|k}=\mathbf{P}_{k|k}^{(N)}$.

Output: $\hat{\mathbf{x}}_{k|k},\mathbf{P}_{k|k}$.

inaccurate ESV and beacon position. In addition, the performance of traditional single beacon navigation method based on the synchronized clock, precise ESV and beacon position[27,30] (to be referred to as "SM"), and the navigation method which can estimate the unknown ESV[10-12] (to be referred to as the "SAM") will also be evaluated as a comparison.

The method of collecting field data can be referred to literature[10-12]. To verify the performance of the proposed method, clock drift and beacon position offset are added in the field data artificially. The clock drift between the beacon and the hydrophone has been set as $\Delta T_k^t = 0.005k\Delta t / 3600$ s, which means the navigation system has a clock-drift of 5 ms per hour. Both beacon position offset Δx_b and Δy_b are set equal to 20 m. When implementing SAM, PM and SM, the following initial settings are selected: (1) 0.5 m/s for the initial v_{cx} and v_{cy} offset, (2) 1520 m/s for the nominal v_e, and (3) $\Delta T_k^{t(0)} = 0$ s for the PM. The tuning parameters of these three methods are: (1) $\sigma_c = 0.01$ m/s, (2) $\sigma_w = 0.1$ m/s, (3) $\sigma_e = 1$ m/s for SAM, (4) $\sigma_{tm} = 0.001$ s, (5) $\sigma_{rm} = 5$ m, (6) $\sigma_{cm} = 0.01$ m/s and (7) 0 m for the nominal beacon position offset. In particular, the iterations N of EM based method is chosen as 15.

The comparison of the estimated trajectories among SAM, PM and SM is shown in Figure 1, together with the true and the nominal beacon position. Similarly, the comparison of horizontal distance error $\Delta_H = \sqrt{(x-\hat{x})^2 + (y-\hat{y})^2}$ among three methods is shown in Figure 2. The Average Root Mean Square (ARMS) of horizontal distance error ARMS Δ_H, defined as:

$$\text{ARMS } \Delta_H = \sqrt{\frac{1}{T}\sum_{k=1}^{T}\left[\left(x_k - \hat{x}_k\right)^2 + \left(y_k - \hat{y}_k\right)^2\right]} \quad \ldots (34)$$

It is also utilized as the evaluation index, in which T represents the total number of fixed sampling intervals. The ARMS Δ_H of SAM, PM and SM are 9.7949, 0.4264, and 24.5856 m, respectively. From Figures 1 and 2 and the comparison of ARMS Δ_H, one concludes that PM has the highest accuracy among these three navigation methods in the presence of unknown clock drift, inaccurate ESV and beacon position. The clock drift utilized in this paper is commonly much bigger than it's actual value

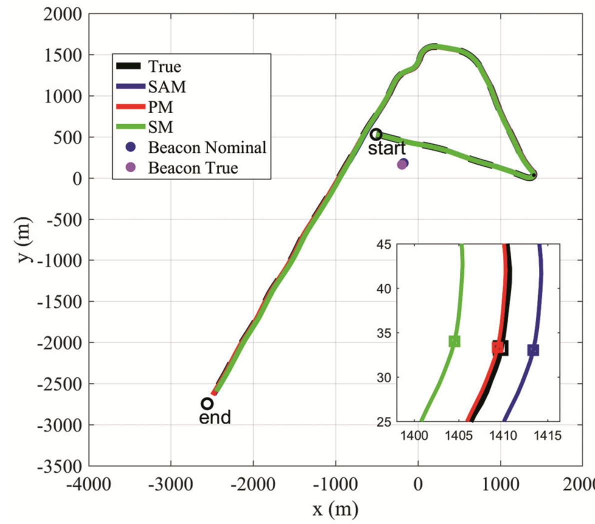

Fig. 1 — Planar position estimates comparison among SAM, PM and SM. The square markers in the sub-graph represent the esti

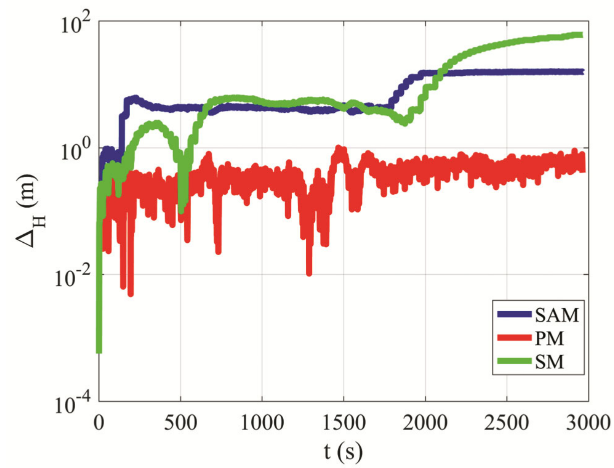

Fig. 2 — Horizontal distance error comparison among SAM, PM and SM

(for instance, the WHOI micro-modem has a average clock drift of 162 microseconds per hour[17]). Even under this unrealistic adverse condition, PM exhibits a satisfactory navigation performance. Because two or three error sources are not considered in SAM and SM, the localization errors of both methods are divergent.

Conclusion

In real applications, the navigation performance of single beacon navigation system was always affected by the unknown clock-drift between the beacon and the hydrophone, as well as the ESV and the beacon position setting error. To eliminate the localization error induced by the unknown clock drift, the imprecise knowledge of the ESV and the beacon position, this paper proposed an EM-based single beacon underwater navigation method, which treated the clock drift, the ESV and the beacon position as unknown system parameters, and estimated these parameters through EM method. Numerical examples using field data indicated that the navigation accuracy of proposed method significantly outperform that of existing state-of-the-art methods in the presence of unknown clock-drift, inaccurate ESV and beacon position.

Acknowledgments

This work was funded by the National Natural Science Foundation of China under Grant 51939003, 51879062 and 52025111.

Conflict of Interest

The authors declare that they have no known competing financial interests or personal relationships that could have appeared to influence the work reported in this paper.

Author Contributions

XY: Conceptualization, Methodology, Validation, Writing - original draft; H-DQ: Conceptualization, Funding acquisition, Project administration; and Z-BZ: Resources, Supervision, Writing - review & editing.

References

1 Kumar S V, Jayaparvathy R & Priyanka B N, Efficient path planning of AUVs for container ship oil spill detection in coastal areas, *Ocean Eng*, 217 (2020) p. 107932.
2 Qin H-D, Yu X, Zhu Z-B & Deng Z-C, An expectation-maximization based single-beacon underwater navigation method with unknown ESV, *Neurocomputing*, 378 (2020) 295-303.
3 Qin H-D, Yu X, Zhu Z-B & Deng Z-C, A variational Bayesian approximation based adaptive single beacon navigation method with unknown ESV, *Ocean Eng*, 209 (2020) p. 107484.
4 Paull L, Saeedi S, Seto M & Li H, AUV Navigation and Localization: A Review, *IEEE J Ocean Eng*, 39 (1) (2014) 131-149.
5 Miller P A, Farrell J A, Zhao Y & Djapic V, Autonomous Underwater Vehicle Navigation, *IEEE J Ocean Eng*, 35 (3) (2010) 663-678.
6 Larsen M B, Synthetic long baseline navigation of underwater vehicles, *OCEANS 2000 MTS/IEEE Conference and Exhibition*, (Providence, RI, USA), 3 (2000), pp. 2043-2050.
7 Lee P, Jun B, Kim K, Lee J, Aoki T, *et al.*, Simulation of an Inertial Acoustic Navigation SystemcWith Range Aiding for an Autonomous Underwater Vehicle, *IEEE J Ocean Eng*, 32 (2) (2007) 327-345.
8 Jin B, Xu X, Zhu Y, Zhang T & Fei Q, Single-Source Aided Semi-Autonomous Passive Location forcCorrecting the Position of an Underwater Vehicle, *IEEE Sens J*, 19 (9) (2019) 3267-3275.
9 Rypkema N R, Fischel E M & Schmidt H, Closed-Loop Single-Beacon Passive Acoustic Navigation forcLow-Cost Autonomous Underwater Vehicles, *2018 IEEE/RSJ Int Conf Intell Robots Syst (IROS)*, (Madrid, Spain), 2018, pp. 641-648.
10 Zhu Z-B & Hu S-L J, Model and Algorithm Improvement on Single Beacon Underwater Tracking, *IEEE J Ocean Eng*, 43 (4) (2018) 1143-1160.
11 Zhu Z-B, Hu S-L J & Li H-J, Effect on Kalman based underwater tracking due to ocean current uncertainty, *2016 IEEE/OES Auton Underw Veh (AUV)*, (Tokyo, Japan), 2016, pp. 131-137.
12 Zhu Z-B, Hu S-L J & Li H-J, Kalman-based underwater tracking with unknown effective sound velocity, *OCEANS 2016 MTS/IEEE Monterey*, (Monterey, CA, USA), 2016, pp. 1-9.
13 Qin H-D, Yu X, Zhu Z-B, Deng Z-C & Tian R-J, Unscented Kalman Filter Based Single Beacon Underwater Localization with Unknown Effective Sound Velocity, *2018 OCEANS - MTS/IEEE Kobe Techno-Oceans (OTO)*, (Kobe, Japan), 2018, pp. 1-6.
14 Yu X, Qin H-D & Zhu Z-B, Globally exponentially stable single beacon underwater navigation with unknown sound velocity estimation, *J Franklin Inst*, 358 (4) (2021) 2515-2534.
15 Deng Z-C, Yu X, Qin H-D & Zhu Z-B, Adaptive Kalman Filter-Based Single-Beacon Underwater Tracking with Unknown Effective Sound Velocity, *Sensors*, 18 (1) (2018) p. 4339.
16 Wolbrecht E, Anderson M, Canning J, Edwards D & Frenzel J, *et al.*, Field Testing of Moving Short-baseline Navigation for Autonomous Underwater Vehicles using Synchronized Acoustic Messaging, *J Field Robot*, 30 (4) (2013) 519-535.
17 Crosbie B P, Anderson M, Wolbrecht E, Canningand J & Edwards D B, Synchronous navigation of AUVs using WHOI micro-modem 13-bit communications, *OCEANS 2010 MTS/IEEE SEATTLE*, (Seattle, WA, USA), 2010, pp. 1-5.
18 Carta D, Optimal Estimation of Undersea Acoustic Transponder Locations, *OCEANS' 78*, (Washington, DC, USA), 1978, pp. 466-471.
19 Pedro B, Long baseline navigation with clock offset estimation and discrete-time measurements, *Control Eng Pract*, 35 (2015) 43-53.
20 Olson E, Leonard J & Teller S, Robust Range-Only Beacon Localization, *IEEE J Ocean Eng*, 31 (4) (2005) 949-958.
21 Arthur D, Natalie L & Donald R, Maximum likelihood from incomplete data via the EM algorithm, *J R Stat Soc*, 34 (1977) p. 39.
22 Thomas B S, Adrian W & Brett N, System identification of nonlinear state-space models, *Automatica*, 47 (1) (2011) 39-49.
23 Ming G & Eric C K, Noise covariance identification for nonlinear systems using expectation maximization and moving horizon estimation, *Automatica*, 77 (2017) 336-343.
24 Vinay A B, Anjali P D & Sachin C P, Identification of process and measurement noise covariance for state and parameter estimation using extended Kalman filter, *J Process Control*, 21 (4) (2011) 585-601.

25 Wahlstrom J, Jalden J, Skog I & Handel P, Alternative EM Algorithms for Nonlinear State-Space Models, *2018 21st International Conference on Information Fusion (FUSION),* (Cambridge, UK), 2018, pp. 1260-1267.

26 Huang Y-L, Zhang Y-G, Xu B, Wu Z-M & Jonathon A C, A New Adaptive Extended Kalman Filter for Cooperative Localization, *IEEE Trans Aerosp Electron Syst*, 54 (1) (2017) 353-368.

27 Gadre S & Stilwell D J, A complete solution to underwater navigation in the presence of unknown currents based on range measurements from a single location, *2005 IEEE/RSJ International Conference on Intelligent Robots and Systems*, (Edmonton, AB, Canada), 2005, pp. 1420-1425.

28 Frandsen P E, Jonasson K, Nielsen H B & Tingleff O, *Unconstrained optimization*, 3rd Edn, Lecture note (Informatics and Mathematical Modelling Technical University of Denmark), 2004, pp. 6.

29 Wilson J R, *Linear system theory*, (Prentice Hall Upper Saddle River, NJ), 1996, pp. 2, 8-9.

30 Casey T, Guimond B & Hu J, Underwater Vehicle Positioning Based on Time of Arrival Measurements from a Single Beacon, *OCEANS 2007*, (Vancouver, BC, Canada), 2007, pp. 1-8.